# Augmented Airbrush for Computer Aided Painting (CAP)

Roy Shilkrot, Pattie Maes, Joseph A. Paradiso and Amit Zoran
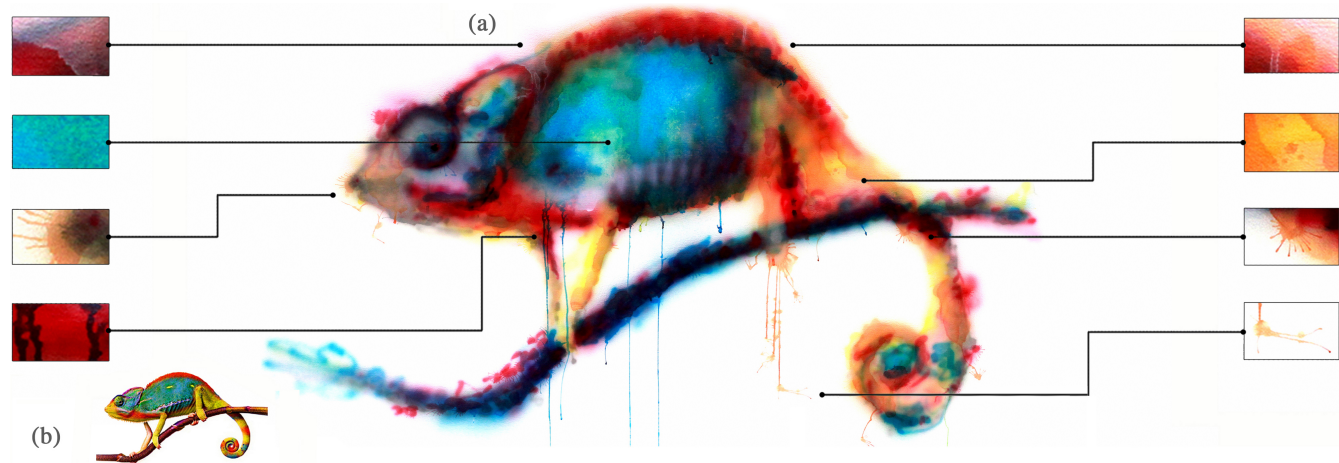Massachusetts Institute of Technology

Fig. 1. Watercolor painting (a) of a chameleon figure (b) using the augmented airbrush, showing unique physical details (canvas width 1.5m, painter A.Z.).

We present an augmented airbrush that allows novices to experience the art of spray painting. Inspired by the thriving field of smart tools, our hand-held device uses 6DOF tracking; augmentation of the airbrush trigger; and a specialized algorithm to restrict the application of paint to a preselected reference image. Our device acts both as a physical spraying device and as an intelligent assistive tool, providing simultaneous manual and computerized control. Unlike prior art, here the virtual simulation guides the physical rendering (*inverse rendering*), allowing for a new spray painting experience with singular physical results. We present our novel hardware design, control software, and a user study that verifies our research objectives.

---

## 1. INTRODUCTION

The plastic arts of painting and sketching have inspired computer graphics (CG) and human-computer interaction (HCI) researchers to find a creative process independent from lengthy acquisition of manual skills. Specifically, the naïve approach of *Paint-by-Numbers* served as a cornerstone for many attempts at creating a manual rendering method with computational assistance [Hertzmann et al. 2001]. Beyond that, some researchers studied the manual styles of skilled graphic artists to enable a virtual simulation of their physical signature [Berger et al. 2013]. However, while researchers acknowledge the value of physical rendering for its authentic, subjective, and chaotic qualities, most of the work in CG simulates these values in a virtual environment, instead of enhancing the physical activity [Baxter et al. 2004].

In recent years, a new research field has been on the rise: smart hand-held tools [Zoran et al. 2014]. The tension between physical creative experience (such as in crafts) and virtual simulation inspired the development of intelligent manual devices. This added a new approach to the combination of digital technology and manual creativity. Building upon this prior art, we present a new smart hand-held tool: an *Augmented Airbrush for Computer Aided Painting (CAP)* that allows unskilled users to render physical paintings and explore the performative and expressive qualities of painting, qualities previously absent from virtual painting.

Unlike a simple paintbrush, the airbrush has at least one mechanical degree of control in its trigger, making it a good platform for augmentation. Airbrushes render blurrier strokes than paintbrushes, as well as morphing colors and smoothing gradients. While these qualities of airbrush painting can be simulated, real-world airbrush painting is an expressive medium, allowing for unrepeatable spray patterns and unique ink staining. Moreover, artists utilize these properties while painting to express their personal style and intentions—qualities that do not pass through the digital reduction of airbrush simulations. The result is a unique artifact, arising
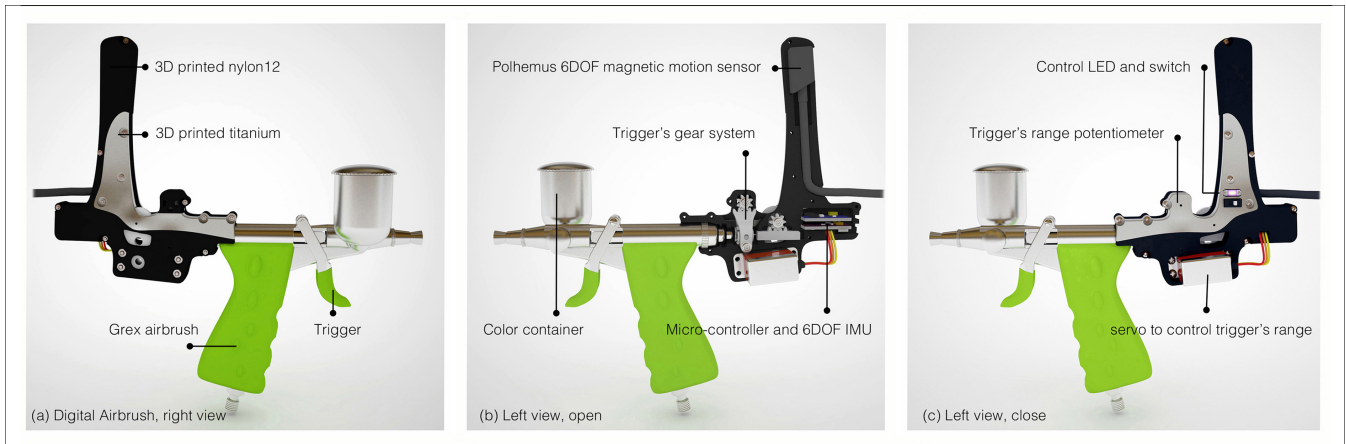
Fig. 2: Augmented airbrush tool. (a) the Grex airbrush with augmentation in black nylon and titanium. (b) an open view of the augmentation reveals the twin gear systems, servo, circuitry and tracking device. (c) closed view shows the LED and switch button.

from these special conditions and the painter's intense investment, which goes beyond the pure graphical qualities.

In this research, we use computational reduction only to assist the user. Unlike the common graphics design process that uses manual input and a virtual canvas to simulate visual data, our *inverse rendering* approach transposes visual data as control to a manual rendering process and a physical canvas, adding new levels of non-simulated complexity to the process.

Our motivation is to enable novice users to render a complex piece while preserving the expressive qualities of their manual practice. Rather than transforming the user into a human copying or printing device, CAP preserves the painting experience and allows for inherently singular, personalized results. This enables users to retain their intuitive responses to variables such as running paint or wet canvas, as part of a wide range of creative visceral action.

To support working in this environment, we developed rapid-response hardware and software elements with a GPU-based algorithm and a light physical model of a paint jet. Using a Motion Magnetic Tracking System (MMTS), virtual history of the painting process, and physical augmentations of the airbrush itself, this hybrid device controls the maximum amount of paint the user can apply to any area of the canvas. In contrast to Paint-by-Numbers, our device supports diffusion of colors and continuous intensity gradients without special modification or markings on the canvas. Moreover, it allows for graphic qualities that are foreign to the simulated world of CG: unique results and singular artifacts, which are possible building blocks for the development of a personal hybrid painting methodology independent of manual skills.

In the next section, we discuss the context for our work and prior attempts to create similar devices. Thereafter we present the technology we developed and methods we used to create the hardware and software for the augmented airbrush. We present the results of both an initial exploration of the capabilities of the device and an extensive user study, before discussing future directions for this research.

## 2. RELATED WORK

**Augmented Expression.** In recent years there has been increasing academic interest in *smart handheld tools* [Zoran et al. 2014], augmented manual devices that assist makers in creative tasks. Examples can be seen in areas of *fabrication* and *sculpting* [Zoran and Paradiso 2013; Rivers et al. 2012; Skeels and Rehg 2007], *sketching* [Yamaoka and Kakehi 2013], and *painting* [Flagg and Rehg 2006]. Within our own work, we wish to use the lessons learned from these new tools to develop a hybrid device, a new *smart tool* in the area of computer assisted graphics.

Computerized assistance in virtual painting, drawing, or sketching has already been extensively researched. While computerized assistance in painting can be implemented in many ways, the prevailing approaches we recognize revolve around *suggestion*, as in ShadowDraw [Lee et al. 2011] or [Eitz et al. 2012]; *tutorial systems* such as [Iarussi et al. 2013; Laviole and Hachet 2012] or Sketch-Sketch Revolution [Fernquist et al. 2011]; and *beautification*, as in [Zitnick 2013], [Limpaecher et al. 2013], and HelpingHand [Lu et al. 2012].

**Digital Airbrushes.** The past decade has seen a number of attempts to create a computer-assisted airbrush device. Most notable are the efforts of [Konieczny and Meyer 2009], who focused on creating a virtual training system for the automotive industry and artistic airbrush painting by using a magnetic tracker and a mock-airbrush device. Joining them in the effort to create a training system are [Yang et al. 2007] and [Kim et al. 2007], who are using augmented reality (AR). However, in contrast to Konieczney, they also incorporated a real spraying device, which was also the goal for [Luk 2004]. Our device, while learning from these attempts, focuses on non-visual instrumented painting through subtle computerized control and also allows for the creation of real paintings as well as virtual simulations.

**Simulating Paint.** We seek to re-introduce physical painting artifacts to the graphic creative practice, as a unique signature of individual users. In the graphics community, researchers have already studied virtual simulation based on real measurements. Lu, DiVerdi [2013] and Xu [2002] present a large body of work that utilizes scannings or models of real brush strokes to interactively generate digital paintings from. Simulation of painting based on models of physical phenomena is another popular field, with work starting as early as Strassman [1986], Curtis [1997], and later in MoXI [Chu and Tai 2005] and IMPaSTO [Baxter et al. 2004]. Our proposed augmented painting device uses a real medium and therefore captures the physical markings of the paper and paint, rather than creating a simulation program.

## 3. INTERACTION AND TECHNOLOGY

To operate our augmented airbrush, the user stands in front of the canvas, free to work on any part of the painting, use any style, and consult the computer screen if he or she wishes (Fig. 3). The reference and canvas are aligned with a calibrated center point that corresponds to the virtual origin. The user can move the device using an organized procedure (sampling the canvas, slicing it, trekking contours, etc.), a more intuitive one (random walking or local focus on a single area), or a mix of both. The computer will intervene only when the virtual tracking corresponds with a paint projection that violates a virtual reference. In such a case, the computer will prevent the user from employing the full potential of the the airbrush trigger (see next section) and applying paint where it is not needed.

Our device is based on a *Grex Genesis.XT*, a pistol-style airbrush, relieved of its rear paint-volume adjustment knob (Fig. 2(a)). Because this is a dual-action airbrush, operating the trigger opens both the pressured air valve and the paint fluid valve, which is made of a needle and a nozzle, resulting in a jet of air mixed with paint particles. We developed a custom-designed augmentation mechanism, which we discuss in the following section, to allow digital control of the paint mixture. A Grex air compressor supplies pressurized air at 20 PSI, and a *Polhemus Fastrack* magnetic motion tracking system positions the device in 6DOF.

### 3.1 Custom Augmentation Hardware

The augmentation module consists of a potentiometer to measure the trigger, a servomotor (servo) to limit the range of the trigger, two gear systems (for the potentiometer and for the servo), and two printed circuit boards (a main controller and an Inertial Measurement Unit[1], or IMU). A 3D printed enclosure connects to the back side of the Grex Genesis.XT and holds the components in place. The major part of this enclosure, as well as the custom gear parts were 3D printed from Nylon12 using a Selective Laser Sintering (SLS) process. Two 3D printed titanium supports were produced in a Direct Metal Laser Sintering (DMLS) process to prevent the user's finger or torque applied by the servo from warping the structure or affecting the position of the magnetic tracking sensor.

The servo gear system implements a paint volume restriction that constrains the linear motion of the original tool's air-fluid mixing needle (Fig 2(b)). The linear controller is driven by a servo (MKS DS95 with ~60ms/60° turn speed at 5v supply) and a gear that translates ~100° of angular motion to 2mm linear motion (covering the full motion range of the trigger). The painter may only pull the needle back with the trigger until blocked by the servo-driven constraint. The system thus provides a digital control that limits the amount of paint fluid mixed with the air jet. However, the user may apply excess force on the trigger and backdrive the servo, overriding the digital control.

A highly accurate sensor detects the user's trigger-pull with a specialized gear mechanism that rotates an angular potentiometer. The original tool's paint-needle lock is fitted with our custom brace, which pushes a gear that translates the needle's 2mm linear motion to 100° rotation (Fig. 2(c)). The angular position is recorded by the potentiometer and sent to the control software at 120Hz. The spring-loaded trigger pulls the needle and our augmentations back

---

[1]The inertial measurement unit, while active and capable of providing a continuous reading, is not currently used in the software. We plan to integrate it in future work to obtain a more accurate position estimation.
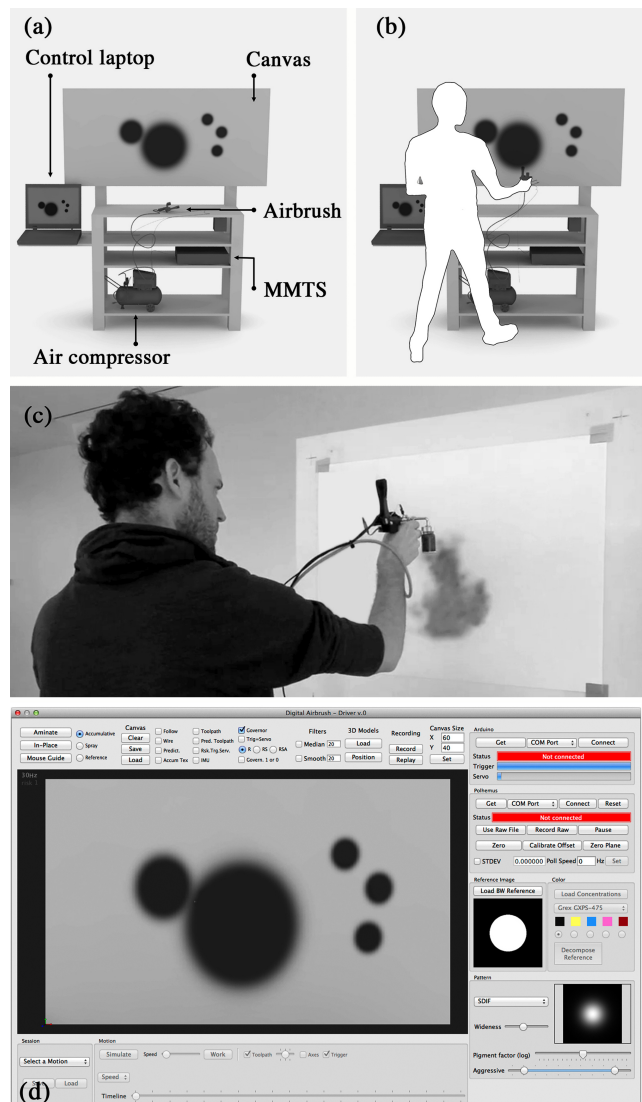


Fig. 3: Interaction modality with the Digital Airbrush. (a), (b) and (c) depict a typical painting session with the augmented airbrush. (d) shows the graphical interface on the companion PC running the simulation.

to their original resting position. We also added an external spring to increase the force of the pull.

3.1.1 *Hardware Integration.* Our tool is fitted with an onboard 8-bit microcontroller (ATMEGA328p-MU) clocked at 16Mhz and a 6DOF inertial measurement unit (MPU-6050), giving it an effective rate of 200Hz (based on the *Femtoduino* PCB layout). The inertial measurement unit, potentiometer, and servo feed into the microcontroller, in turn, and are driven by the USB power supply. The firmware polls the sensors (inertial measurement and potentiometer) at 120Hz and uses a 3-value median filter to eliminate noise, as well as a linear low-pass filter. The signal from the control software on the PC drives commands to the servo at 120Hz. However, assuming a worst-case scenario, the servo must turn 120° at once, which will take ~120ms. This means that it must work at an effective frequency of ~10Hz or ~8% of the original signal. Therefore, an 11-tap low-pass linear filter is used to keep the la-

tency within an acceptable range of the servo; this filter is also used to filter the potentiometer signal.

## 3.2 Physical Model

Baxter et al. [2004] were among the first to implement a physical simulation-driven virtual brush, taking into account numerous parameters (i.e. paint advection and absorption). However, this system and other simulation methods require intense computational resources, while ours targeted a 100-120Hz frame-rate. Alternatively, [Deussen et al. 2012] used computer vision to track the status of the paint on the canvas. However, because this method does not give a prediction of jet distribution as a function of the user's action, it cannot be used for trigger control.

In order to enable fast reaction and accurate prediction, we designed an approximate paint jet distribution model based on a lookup table and the parameters of the tool's position and trigger state. While developing this model, we performed several motionless tests (where the tool's position does not change while the trigger is opened, see Fig 4). Many of the open parameters are constrained: air pressure (20 PSI), tool's angle to canvas (set as perpendicular to canvas), paint mixture (10% weight diluted Carbon Black), paper (a drawing paper with minimal absorption rate), and environment (no air draft, fixed humidity and temperature). The parameters available for modeling are the tool's distance from the canvas ($d$), the radial distance from of the center of spray projectile ($r$), the value of the trigger (Trig), and the duration of the spray ($t$).

In total, we performed six tests, each at a different distance from the canvas, for varying spraying durations and trigger pressure values. The appearance of paint on the canvas was recorded using an HD video camera (60 FPS). During the post-processing stage, the visual data was normalized, aligned, and registered (Fig. 4(a-b)). Since we are looking for differential data, such that a given moment will tell how much paint *is added* to the canvas, the data was differentiated with respect to time. The pigment drying rate, which affects its perceived intensity, was modeled with a linear function based on additional measurements taken from paint that we left out to dry.

Our analog 3D Spray Differential Intensity Function (analog SDIF) represents the paint intensity increment given $d, r$ and $t$ (see Fig. 4(c)). The trigger value (Trig) and the elapsed time ($d$Time) are external factors. Thus, the additive spray for time $k + 1$ is:

$$\text{Spray}[i]_{k+1} = d\text{Time}_k * g(\text{Trig}) * \text{SDIF}(r, d, t_k) \quad (1)$$

$$\text{Int}[i]_{k+1} = \text{Int}[i]_k + \text{Spray}[i]_{k+1} \quad (2)$$

$$g(\text{Trig}) = 1 - \text{Trig}^2 \quad (3)$$

In our model, the time $t$ spent spraying a texel $i$ is proportional to its intensity $\text{Int}[i]$ through the SDIF. Therefore, $t$ can be obtained from the current intensity $\text{Int}[i]$ via an inverse function that essentially codes how long ($t$, in seconds) it takes the texel $i$ to reach the intensity $\text{Int}[i]$. Thus, the Inverse Temporal Spray Function (ITSF) is written (Fig. 4(d)):

$$t_k = \text{ITSF}(r, d, \text{Int}[i]) \quad (4)$$

The SDIF and ITSF are sampled and saved as 512x512x16 3D textures in the GPU; they serve as a lookup table for the shaders.

The trigger mechanically controls the position of the internal mixture needle, which in turn blocks or clears the orifice of the circular nozzle to let paint mix with the jet of air. A rough approximation of the trigger's impact on the pigment saturation is a parabolic function of its linear translation (see eqn. 3), since at the point of blockage the area of the nozzle orifice is $\pi r_o^2$ and the area



(a)

(b)

6.4sec 152mm    20sec 285mm    2sec 107mm    35cm

20sec 203mm    14.5sec 178mm    1.9sec 114mm    0cm

(c)

Distance from canavas
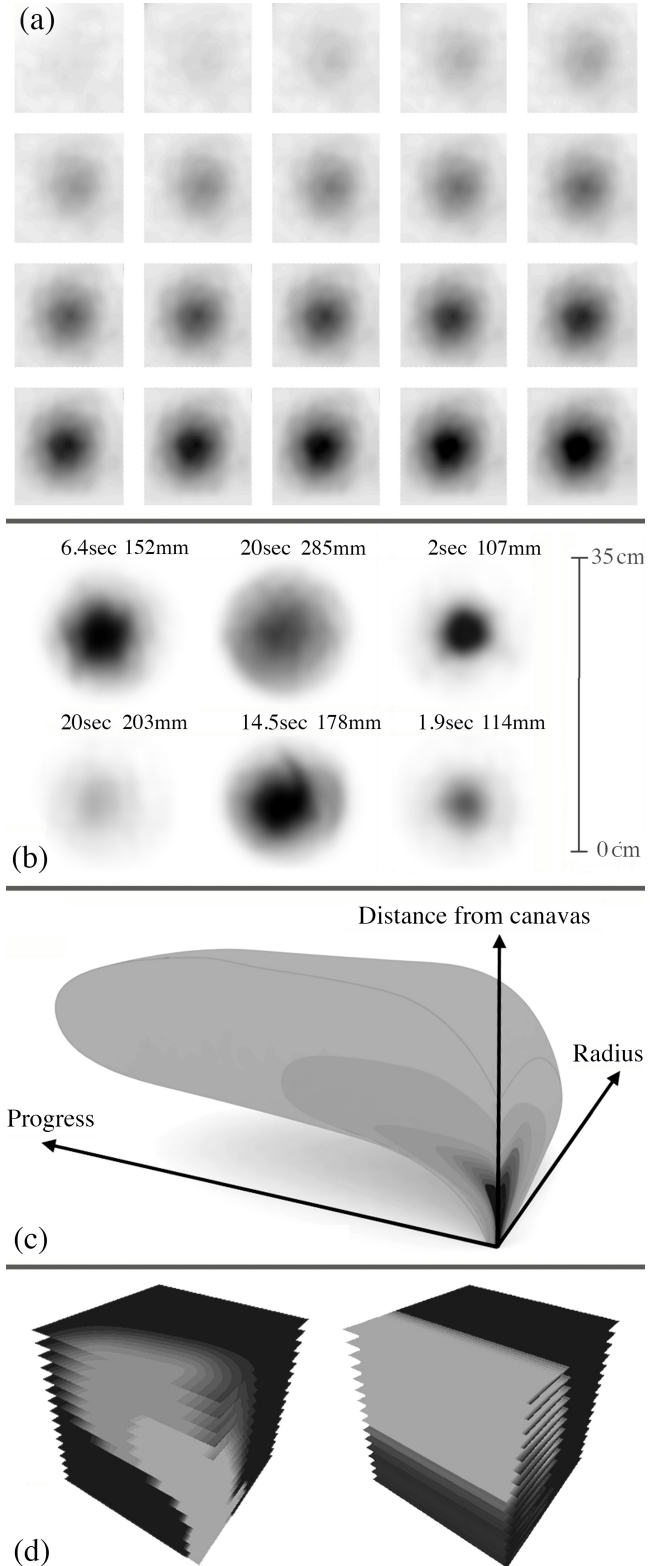
Radius

Progress

(d)

Fig. 4: Spray physical model. (a) equidistant samples of spray distribution (100msec between samples), (b) aligned spray measurements, (c) illustration of the analog SDIF, and (d) the sampled SDIF and ITSF as represented in the GPU as 3D textures.
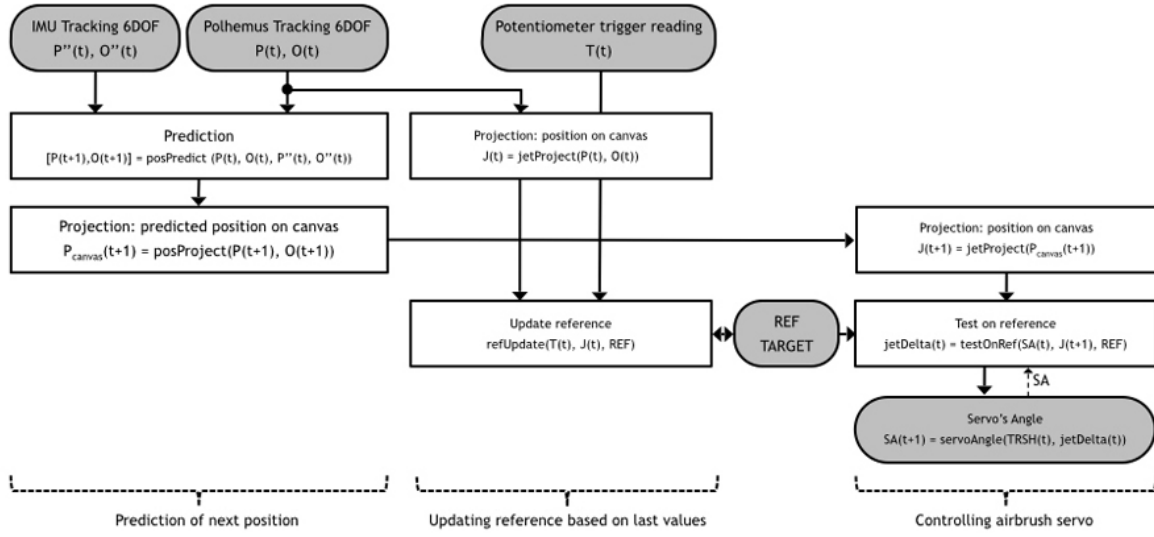
Fig. 5: The control algorithm, flow diagram. Dark rounded boxes are inputs/outputs in the system, and bright straight boxes represent computation points.

that the needle occupies is $\pi r_i^2$. Therefore, the remaining open area is $\pi(r_o^2 - r_i^2)$ where $\pi$, $r_o$ are constants.

## 3.3  Software

We designed the software to enable realtime tactile feedback to the painter. It has been divided into a number of threads executing in parallel, to maximize usage of the CPU cores and GPU. The system is time-driven at the rate of measurements coming from the tracking system, ~120Hz. These measurements are used to find the impact of the spray on the canvas, derive the risk to the work, and determine what the tool's reaction should be, all while maintaining an up-to-date simulation of the canvas (Fig. 5). The software allows users to choose the reference image, set the risk calculation parameter and calibrate the physical and virtual canvas. After calibrating the canvas, users can initiate the governor that controls the tool.

### 3.3.1  Tracking, Filtering, Predicting and Signaling. A software thread is governed on collecting a 6DOF position measurement for the brush tip at 120Hz from the magnetic tracker. For noisy environments, it optionally applies a median filter or linear low-pass filters of varying sizes. Additionally, to compensate for the servo's lag, a future estimate of the brush position is created from a 4th-order Bézier spline extrapolation. The position measurement stream is then filtered to a 20Hz signal that matches the speed of the servo's response time.

After the risk-level calculation, which will be discussed shortly, commands are fed to the servo via the microcontroller in another thread, which also polls for inertial information (acceleration and orientation) and obtains the trigger's position. See Fig. 5 for a data-flow diagram.

### 3.3.2  Calibration. Since the position of the tracking sensor is not where the paint-jet is originating from, an offset vector must be calculated. To do so, a large number of samples taken from the position and orientation of the sensor are collected around a fixed point. The samples lay on a sphere, which is centered on the fixed position of the nozzle. Therefore, a spherical model is fit to the data (four parameters) with a gradient descent algorithm based on

the distance of each sample from the surface of the sphere. Once the central point is obtained, the offset can be calculated and fixed in relation to the frame of the sensor, because the sensor and nozzle are embedded in the same rigid object. The same algorithm is used to find a minimally fitting three-parameter model of the offset.

To calibrate the working canvas, the system collects a large number of position samples on the canvas by instructing the user to slide the nozzle across the surface to its corners. Assuming a planar surface for the canvas, PCA is performed on the data and obtains the normal to the surface, as well as the mean point, which is regarded as the offset of the canvas' center from the origin.

The potentiometer and servo were manually calibrated to span the linear motion required to constrain or detect the volume of pigment, mapping the values to the $[0, 100]$ range for simplicity.

### 3.3.3  Canvas Rendering. After receiving information on the position in space of the airbrush and its trigger, the system estimates the amount of paint that will hit the canvas. The aforementioned model of incremental paint is used, utilizing the trigger pressure and distance from the surface. The canvas is represented as a floating point texture that holds in each texel the paint cover on that portion of the mesh.

The accumulated paint on the virtual canvas is compared with a reference texture to determine, per texel, if more paint should be allowed to accumulate in that location or if it has reached saturation. The per-texel risk measure is summed up over the entire canvas to get a global risk factor, which in turn translates to servo commands:

$$\text{servo} = 1 - \text{Aggression} * \frac{\sum_i \text{RefSub}[i]}{\sum_i \text{Spray}[i]} \qquad (5)$$

$$\text{RefSub}[i] = \text{Ref}[i] - (\text{Int}[i] + \text{Spray}[i]_{\text{prediction}}) \qquad (6)$$

To provide a consistent measure of risk through different scales (as the distance of brush from surface creates a larger spread), the reference image subtraction is normalized with the total amount of spray reaching the canvas. The user determines the aggression parameter, which can affect how the computation regards the risk. All of these operations are implemented on the GPU in vertex and fragment shaders.
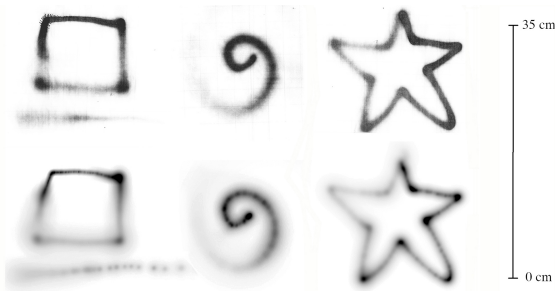
Fig. 6: Spray model sanity tests. Top: Scannings of the canvas. Bottom: Computer simulations using our model.

## 4. INITIAL EXPLORATION AND COLOR

In this section, we present several experiments we conducted with our airbrush: the accuracy and tracking test leads to monochromatic, bichromatic, and full-colored paintings. A basic MSE test of the tracking system provides a general evaluation of the impact of the servo and the steel body of the airbrush on the magnetic tracking ($\sigma = 0.25$mm in a 2-second motionless measurement, $\sim$240 data points). Simple primitive free-hand gestures were performed to visualize the accuracy of our physical model using a Carbon Black pigment, comparing the virtual simulation and the manual interaction (see Fig. 6).

### 4.1 Monochromatic painting

We began our painting experimentation with a semi-monochromatic work (again with the Carbon Black pigment) and a contrastive greyscale reference image. Unlike the development of the physical model, where we used a paper with a minimal absorption rate, here we moved to a watercolor paper with a higher absorption rate (*Arches Watercolor Paper* 140lbl). The panda painting (Fig. 7(a)) resembles a Paint-by-Numbers method, to test the trigger responsiveness to sharp edges and covering surfaces (see Fig. 7(b) for the simulated paint and Fig. 7(c) for a photograph of the real painting). This early example already demonstrates the appearance of unique physical artifacts. When the device approaches the surface of the paper, a concentrated air jet presses the wet paint before it dries on the paper to create an "explosion-like" artifact.

A more advanced example is presented in Fig. 7(d-f), with the elephant painting project. This painting demonstrates working with smoother grayscale gradients, while recreating complex shaded surfaces and scene depth. Working on this example, we constantly changed the model aggression parameters to achieve a visually satisfying result. An initial reflection is that although our driver and physical model performed well, spray painting is an interactive process that requires the user to constantly evaluate the progress and adapt the work to attain a subjectively satisfying output.

### 4.2 Multi-pigment painting

To allow painting with more than one pigment, we implemented a number of algorithms to simulate the mixture of layers of sprayed pigments, based on a derivation of the Kubelka-Munk (K-M) theory from [Konieczny and Meyer 2009; Baxter et al. 2004]. Our goal was to take a reference image and decompose it into layers of pigment, given the predetermined palette of pigments that we obtained. For our pigments—Phthalocyanine Blue, Naphthol Red, Arylide Yellow and Carbon Black—we obtained scatter (S), absorption (K), reflectance , and transmittance (T) spectral measure-
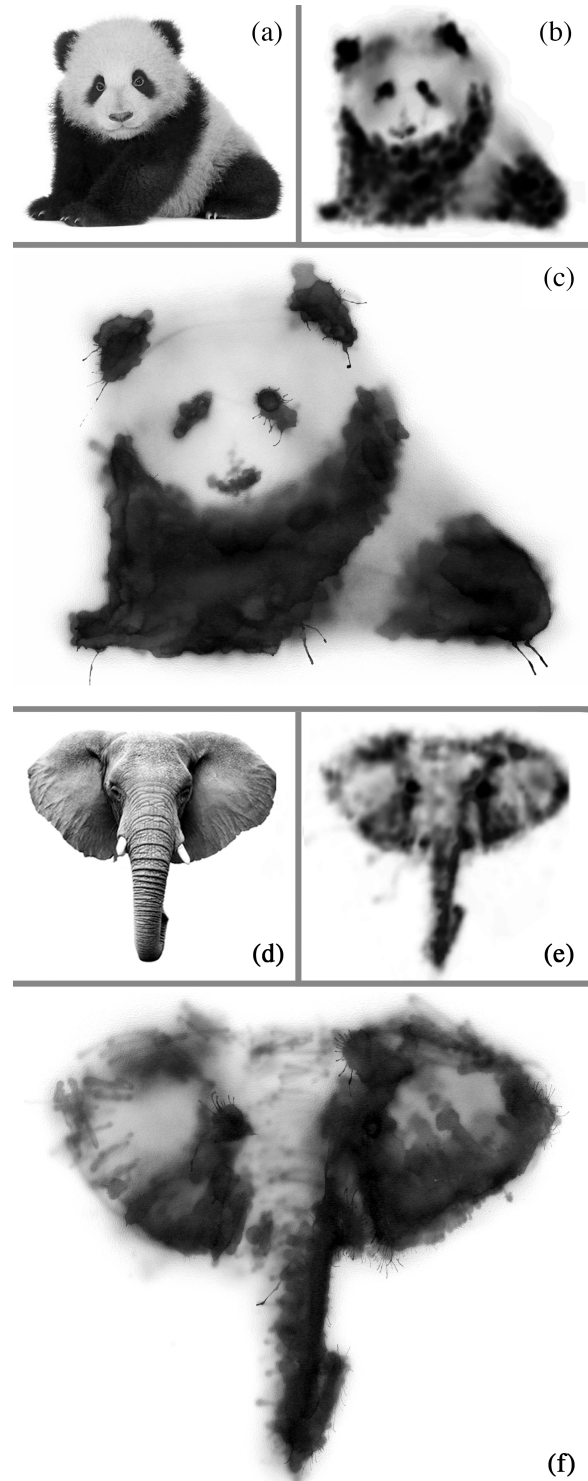


Fig. 7: Monochromatic painting of panda and elephant (painter: A.Z.). (a) The reference image of a panda, (b) a virtual simulation of the painting session, and (c) a photograph of the final result (canvas width 0.8m). (d) The reference image of an elephant, presenting grayscale gradients and complex surfaces, (e) a simulation of the painting session and (f) a photograph of the canvas (canvas width 0.8m).

ments from the LBNL pigment database [Levinson et al. 2014], as required by the K-M equations. Since all of our colors are transparent and water-based, the simpler *complete hiding* K-M equations [Haase and Meyer 1992] do not hold. Rather, the general equations that account for the thickness of the pigment layer must be used. As there are a number of forms, the K-M equations may be written. This is the formulation that we used:

$$KS = K_\lambda/S_\lambda \tag{7}$$

$$b = \sqrt{KS(KS + 2.0)} \tag{8}$$

$$R_\lambda = \frac{1}{1 + KS + b/\tanh(bS_\lambda d)} \tag{9}$$

$$T_\lambda = \frac{bR_\lambda}{\sinh(bS_\lambda d)} \tag{10}$$

$K_\lambda$ and $S_\lambda$ are the scatter and absorption for a given wavelength ($\lambda$), and $d$ is the thickness of the pigment layer. A 60-wavelength numeric representation for the spectral information is used in the calculations (400-700nm range, with 5nm steps). For the mixture of pigments, we used the incremental formulas from [Konieczny and Meyer 2009].

After converting the input image to CIEXYZ, we calculated the thicknesses of the four pigment layers that best represent the pixel color. Hasse and Meyer [1992] used a gradient descent optimization scheme to solve for the pigment concentrations for a single color in *complete hiding*, employing closed-form formulas for the partial derivatives. Our implementation uses a brute-force color matching scheme, with a precalculated 4D grid of the combinations of pigments (starting from a white background, D65 standard illuminant) and a coarse-to-fine parallel process to achieve reasonable running times for this offline process (a 750x750 pixel image is decomposed to four pigment layers in ~200 seconds). For matching the input and precalculated colors, we used the L*a*b* colorspace distance measure from [Haase and Meyer 1992]: $\Delta E = \|A_{Lab} - B_{Lab}\|_2$. Once the pigment layers have been obtained, each layer is treated as a single pigment spraying session, and the thickness measures are used as the reference for the program.

The tiger painting (Fig 8(a-d)) shows a basic use of two colors, Arylide Yellow and Carbon Black, on a cotton canvas (the only paint on cotton canvas within this paper). The frog project (Fig 8(e-k))) integrates all four colors—Phthalocyanine Blue, Naphthol Red, Arylide Yellow and Carbon Black—and an additional orange made by mixing the Naphthol Red and Arylide Yellow (using boolean operations between the red and yellow references).

Finally, the chameleon (Fig 1) project demonstrates an interactive physical painting process, where we used a white opaque color to eliminate parts of the painted work and erased the simulated reference before re-layering the canvas. This process, using multiple layers and an explorational mixing of colors (replacing blue with green and red with orange without updating the reference, as with the chameleon painting), contributes a depth and complexity of layers, textures, and colors.

## 5. TECHNICAL LIMITATIONS

While the airbrush device performed well during the paintings presented in this paper, as well as the user study discussed in the next section, there are several technical limitations to address in future design iterations. For example, since the physical model is not a complete physical simulation of the air and pigment-water fluids, it does not simulate paint advection or run-offs. On the other hand, our model can *detect* run-offs risk if it reaches saturation.
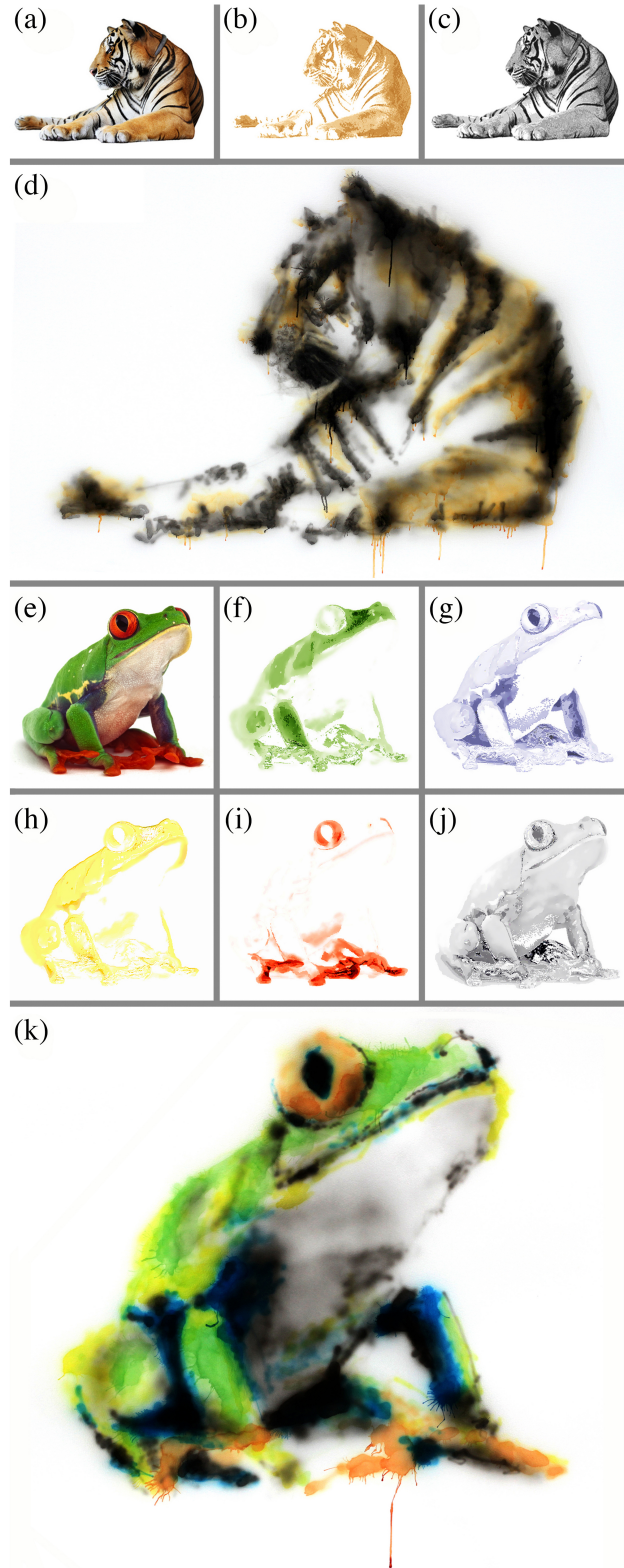


Fig. 8: (a-d) Multi-pigment painting of a tiger (canvas width 1.5m). (e-k) Multi-pigment painting of a frog (canvas width 1m). Painter: A.Z.
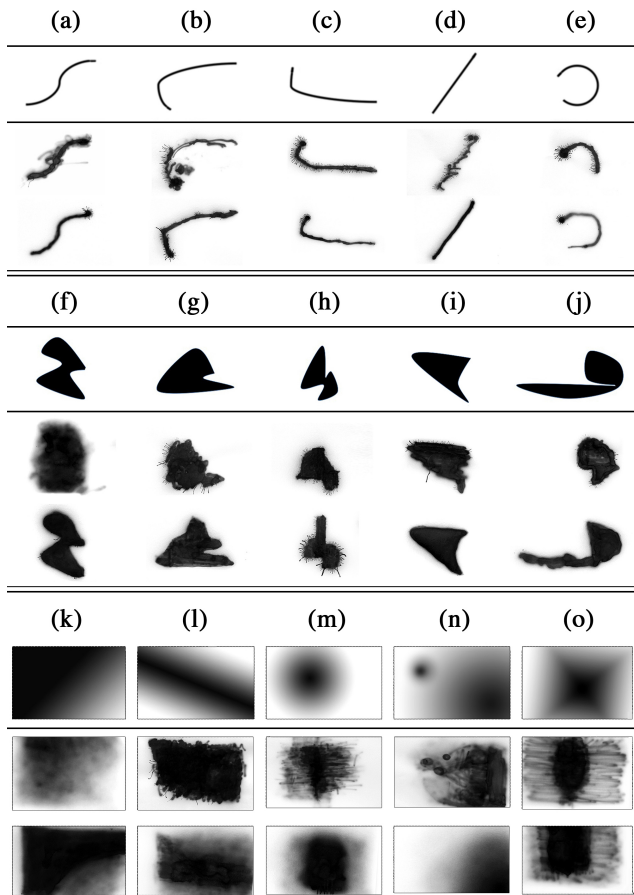
Fig. 9: Painting results from the user study. (a)-(e) Curves. (f)-(j) Shapes. (k)-(o) Gradients. The top line in each category shows the reference, the middle line shows our participants' results from the first day, and the bottom contains the results from the fifth day. We can identify an obvious improvement in execution.

As mentioned earlier, the Grex Genesis.XT airbrush is a dual action airbrush, in which the trigger action opens both the pressured air valve and the paint fluid valve. A drawback of this design is that when a user squeezes the trigger only lightly, while the paint fluid valve is still closed, a small amount of paint still seeps through it. Although the pigment density in such a case is very low, our mechanical constraint cannot entirely prevent overriding the reference, so the results depends on the user's dexterity. In addition, the servo reaction time (0.066 sec/60 degrees with no load) and torque (2.44 kg-cm) cannot guarantee immediate and absolute restraint of the paint jet when going quickly over edges, especially if the user applies excessive force. Moreover, allowance of painting near sharp edges, as controlled by the risk factor, may cause extra blurriness. However, this can also be seen as a quality associated with airbrush painting in general, and not only with our system.

## 6. USER STUDY

The objectives of the user study are twofold. First, we wish to evaluate to what extent the device can deliver spatial information on the required painting solely using the trigger augmentation. In addition, we wish to evaluate the quality of this experience, extrapolating

recommendations for future work and understanding the learning curve of the interaction.

We recruited five volunteers with no prior skills in spray painting or any other form of painting, sketching or drawing, and asked them to repeat similar painting procedures over five days. Before the study we allowed each subject to familiarize him- or herself with using the device on sacrificial paper, guided by the cues that it provides. On each day of the study, the participants were asked to paint until they were satisfied with the result with no time constraints. On average, it took them 30 to 60 minutes to complete the tasks, followed by a 5-minute verbal interview. All free parameters of the software were set and locked throughout all the tasks.

We prevented any information about the reference from appearing in any channel except the trigger, to evaluate whether the trigger by itself can deliver spatial guidance. According to this goal, tasks were designed for curves, complex shapes and gradients (see Fig. 9). The nature of the task was verbally described to the participants, but they could see neither the reference nor any other type of assistance. Participants painted five different references per task, however the task sequence was changed per user, to prevent a procedural bias.

To add quantitative measurements to our qualitative evaluation of the painting we asked Amazon Mechanical Turk voters to identify each single task result out of a selection of ten possible matches (including the five original references and an additional five). The total number of quality measurements (i.e. votes) was 4,500, comprising sixty votes per seventy-five tasks (five users over five days, each completing three tasks per day). Every vote was converted to a binary test—successful identification or non-successful identification—and the binary tests were uniformly converted to an average $[0, 1]$ score (0 means failure to identify while 1 means success). The success of our participants in recreating the references was measured according to that score. The results of the aggregated voting data suggest that the study participants slightly improved at all the tasks we examined. See Fig. 10 for the results in graph form.

### 6.1 Discussion: Haptic Feedback and Mental Model

Through observing the participants' work and the daily summative interviews, we discovered that they developed several strategies to locate shapes and execute them. The two most prominent strategies were: *dotting-then-filling*, and *filling-then-stopping*. In the dotting-then-filling strategy, the users dotted the outline of the shape or line using the cues, and once the edge was obvious they used broad, confident strokes to fill it in. The filling-then-stopping strategy was when the users started from a location inside the shape and simply moved in any direction until they got a cue to stop, repeating this procedure until it resulted in a filled shape or line. In general, the dotting strategy, which was used by all but one of the participants, resulted in cleaner executions. While working on the gradients, most of the participants opted for the fill-then-stop strategy to make out the gradual fall of intensity.

The augmented airbrush delivers 1D haptic information through its trigger, allowing or disallowing the application of paint on the canvas. To reconstruct a continuous spatial mental model of an unknown graphical reference, a user must sample the space while understanding the feedback behaviour of the device. Participants reported that they experienced the most significant improvement in this operation between the first and second day, reaching a stasis in the last two days. Users also commented that the most difficult part of each task was finding and keeping a *global* mental model while using the *local* reading from the tool.
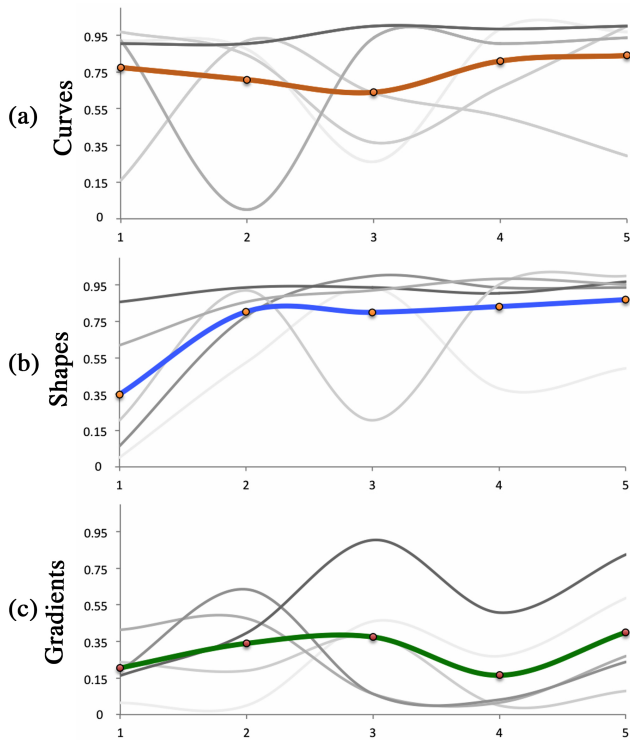
Fig. 10: Results of the user study as evaluated by Amazon's Mechanical Turk voters. Gray lines represent the scores individual users received for a given task through the days of the study; colored lines are the average.
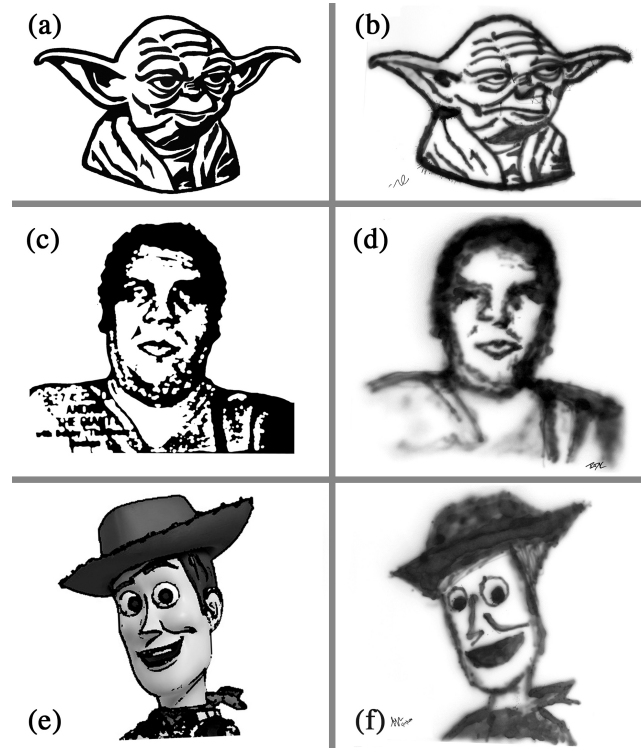


Fig. 11: Work of three of the study participants beyond the tasks. Each row presents the work of a different participant, where the left image is the reference and on the right is their execution. (a) Star Wars © & ™ 2014 Lucasfilm Ltd. All rights reserved. Used under authorization [Yoda's Datapad 2014]. (e) Source [Toy Story Wallpapers 2014]

In the case of low-degree graphic complexity, the data suggest that users successfully satisfy the juried recognition test. Their curves recognition scores were high even on the first day. For the more complex task of shapes, they obtained similar results from the second day on. Obtaining a mental model was more difficult when the reference included gray scale rather than only binary data, as hinted by the lower scores on the gradient tasks (Fig. 9(k-o) and 10(c)). While the scores may suggest an improvement even in this area, they are somewhat noisy and cannot support a strong claim of improvement on these tasks.

A close look at (Fig. 9(a)-(e)) shows significant improvement in the execution from the first day to the last, although the Mechanical Turk evaluation (Fig. 10(a)) shows only an incremental improvement in recognition (probably since it already starts with high scores). In the infinite space of possibilities for curves and shape, a handful of successful samples of the reference shape provide the painter with enough spatial information to recreate a "recognizable" painting, if not a high quality one. However, the quality of the drawing gets better as participants develop a more solid understanding of the goal. As they improve in skill and confidence, they are able to construct smoother and more saturated results. Moreover, participants commented that while the interaction first felt uncanny, it soon became enjoyable after gaining experience in the hybrid interaction, as one stated: "on the one hand, I was "reading" the tools' instruction, but on the other hand I was writing with my own style."

After the study ended, three of the participants opted to paint an image of their choosing. We observed a varying degree of reliance on the cues from the tool or overriding the guidance by forcing the trigger or spraying very lightly (as discussed in Section 5). While

Fig. 11(b) shows a careful execution with close adherence to the reference, Fig. 11(d) already demonstrates usage of gradients and blurriness that were not part of the reference, but a result of the painter's choice. In Fig. 11(f), where the painter again used the dotting method, we can see that the result is a projection of the painter's mental model of the reference and overriding, rather than a careful implementation of the reference (see Fig. 11).

In the common case, when users can look at the reference during the painting process, they use the device only for spatial wayfinding, similar to the examples by the authors shown earlier (Fig. 7 and 8). We conclude that in general, while the five-day study shows high success in guiding users in simple drawing tasks, it is more difficult to reconstruct mental models for complex references.

## 7. CONCLUSION

We presented an augmented airbrush device, including custom hardware and an algorithm allowing for realtime trigger augmentation. Unlike visual augmented reality methods to assist novices in complex tasks, our approach keeps the user's attention on the handheld painting device and the physical canvas.

The digital airbrush allows the users to experience the manual painting process, with the unique physical artifacts of the results. A user study verified that the device successfully supports novices in providing spatial information without any visual cues, with the participants' work showing an improvement in quality over five days.

We demonstrated that the device recaptures graphic qualities that complement existing computer simulations—unique results and singular artifacts, representing realtime physical conditions of air-
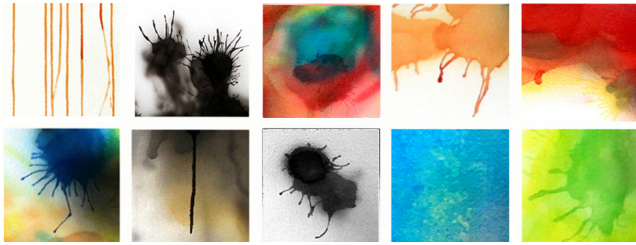
Fig. 12: Unique and unpredicted qualities of real spray painting: diffusion, running paint, saturated paper and other artifacts.

brush painting (Fig. 12). While details such as runny paint or blurry edges modify and personalize the references, the final painting may still closely resemble the original, though it was created by an unskilled painter.

This work is a direct extension of a growing portfolio of smart hand-held tools that contest traditional HCI paradigms of virtual and physical user experience. While many graphics research projects aim to add authenticity to the results by simulating chaotic and semi-chaotic artifacts of the traditional painting practices, we contribute a methodology where both manual engagement and virtual assistance are unified in a single creative process. We believe our path may lead to the development of personal hybrid painting agendas independent of manual skills.

## 8. ACKNOWLEDGMENTS

## REFERENCES

BAXTER, W. V., WENDT, J., AND LIN, M. C. 2004. IMPaSTo: a realistic, interactive model for paint. In *Proc. of NPAR*, S. N. Spencer, Ed. NPAR '04. ACM, Annecy, France, 45–56.

BERGER, I., SHAMIR, A., MAHLER, M., CARTER, E., AND HODGINS, J. 2013. Style and abstraction in portrait sketching. *ACM Trans. Graph. 32,* 4 (July), 55:1–55:12.

CHU, N. S.-H. AND TAI, C.-L. 2005. MoXi: real-time ink dispersion in absorbent paper. In *ACM SIGGRAPH 2005 Sketches*. SIGGRAPH '05. ACM, New York, NY, USA.

CURTIS, C. J., ANDERSON, S. E., SEIMS, J. E., FLEISCHER, K. W., AND SALESIN, D. H. 1997. Computer-generated watercolor. In *Proc. of SIGGRAPH*. SIGGRAPH '97. 421–430.

DEUSSEN, O., LINDEMEIER, T., PIRK, S., AND TAUTZENBERGER, M. 2012. Feedback-guided stroke placement for a painting machine. In *Proceedings of the Eighth Annual Symposium on Computational Aesthetics in Graphics, Visualization, and Imaging*. Eurographics Association, 25–33.

EITZ, M., HAYS, J., AND ALEXA, M. 2012. How do humans sketch objects? *ACM Trans. Graph. 31,* 4 (July), 44:1–44:10.

FERNQUIST, J., GROSSMAN, T., AND FITZMAURICE, G. 2011. Sketch-sketch revolution: An engaging tutorial system for guided sketching and application learning. In *Proc. of UIST*. UIST '11. ACM, New York, NY, USA, 373–382.

FLAGG, M. AND REHG, J. M. 2006. Projector-guided painting. In *Proc. of UIST*. UIST '06. ACM, New York, NY, USA, 235–244.

HAASE, C. S. AND MEYER, G. W. 1992. Modeling pigmented materials for realistic image synthesis. *ACM Trans. Graph. 11,* 4 (Oct.), 305–335.

HERTZMANN, A., JACOBS, C. E., OLIVER, N., CURLESS, B., AND SALESIN, D. H. 2001. Image analogies. In *Proc. of SIGGRAPH*. SIGGRAPH '01. ACM, New York, NY, USA, 327–340.

IARUSSI, E., BOUSSEAU, A., AND TSANDILAS, T. 2013. The drawing assistant: Automated drawing guidance and feedback from photographs. In *Proc. of UIST*. UIST '13. ACM, New York, NY, USA, 183–192.

KIM, D., YOON, Y., HWANG, S., LEE, G., AND PARK, J. 2007. Visualizing spray paint deposition in VR training. In *Virtual Reality Conference, 2007. VR '07. IEEE*. 307–308.

KONIECZNY, J. AND MEYER, G. 2009. Airbrush simulation for artwork and computer modeling. In *Proc. of NPAR*. NPAR '09. ACM, New York, NY, USA, 61–69.

LAVIOLE, J. AND HACHET, M. 2012. PapARt: interactive 3D graphics and multi-touch augmented paper for artistic creation. In *3D User Interfaces (3DUI), 2012 IEEE Symposium on*. 3–6.

LEE, Y. J., ZITNICK, C. L., AND COHEN, M. F. 2011. ShadowDraw: real-time user guidance for freehand drawing. *ACM Trans. Graph. 30,* 4 (July), 27:1–27:10.

LEVINSON, R., BERDAHL, P., AND AKBARI, H. 2014. Lawrence berkeley national laboratory pigment database.

LIMPAECHER, A., FELTMAN, N., TREUILLE, A., AND COHEN, M. 2013. Real-time drawing assistance through crowdsourcing. *ACM Trans. Graph. 32,* 4 (July), 54:1–54:8.

LU, J., BARNES, C., DIVERDI, S., AND FINKELSTEIN, A. 2013. RealBrush: painting with examples of physical media. *ACM Trans. Graph. 32,* 4 (July), 117:1–117:12.

LU, J., YU, F., FINKELSTEIN, A., AND DIVERDI, S. 2012. HelpingHand: example-based stroke stylization. *ACM Trans. Graph. 31,* 4 (July), 46:1–46:10.

LUK, J. 2004. Computer-controlled airbrush with motion tracking. Tech. rep., University of British Colombia, Vancouver, B.C. Canada. Apr.

RIVERS, A., ADAMS, A., AND DURAND, F. 2012. Sculpting by numbers. *ACM Trans. Graph. 31,* 6 (Nov.), 157:1–157:7.

SKEELS, C. AND REHG, J. M. 2007. ShapeShift: a projector-guided sculpture system. UIST.

STRASSMANN, S. 1986. Hairy brushes. In *Proc. of SIGGRAPH*. SIGGRAPH '86. ACM, New York, NY, USA, 225–232.

TOY STORY WALLPAPERS. 2014. `http://www.toystorywallpapers.com/wp-content/uploads/wallpapers/woody_headshot_toy_story_3_wallpaper_-_1600x1200.jpg`.

XU, S., TANG, M., LAU, F., AND PAN, Y. 2002. A solid model based virtual hairy brush. In *Computer Graphics Forum*. Vol. 21. Wiley Online Library, 299–308.

YAMAOKA, J. AND KAKEHI, Y. 2013. dePENd: augmented handwriting system using ferromagnetism of a ballpoint pen. In *Proc. of UIST*. UIST '13. ACM, 203–210.

YANG, U., LEE, G., SHIN, S., HWANG, S., AND SON, W. 2007. Virtual reality based paint spray training system. In *Virtual Reality Conference, 2007. VR '07. IEEE*. 289–290.

YODA'S DATAPAD. 2014. `http://www.yodasdatapad.com/livingroom/fanworks/art/landon/yoda.html`.

ZITNICK, C. L. 2013. Handwriting beautification using token means. *ACM Trans. Graph. 32,* 4 (July), 53:1–53:8.

ZORAN, A. AND PARADISO, J. A. 2013. Freed: a freehand digital sculpting tool. In *Proc. of CHI*. CHI '13. ACM, 2613–2616.

ZORAN, A., SHILKROT, R., GOYAL, P., MAES, P., AND PARADISO, J. 2014. The wise chisel: The rise of the smart handheld tool. *Pervasive Computing, IEEE*.